Rapid Communications

Bloch oscillations with a metastable helium Bose-Einstein condensate

R. F. H. J. van der Beek,[1] O. Onishchenko,[1,*] W. Vassen,[1,†] K. S. E. Eikema,[1] and H. L. Bethlem[1,2]

[1]*LaserLaB, Department of Physics and Astronomy, Vrije Universiteit, De Boelelaan 1081, 1081 HV Amsterdam, Netherlands*

[2]*Van Swinderen Institute for Particle Physics and Gravity, University of Groningen, Groningen, Netherlands*

(Received 4 August 2020; revised 20 November 2020; accepted 20 November 2020; published 21 December 2020)

We have observed Bloch oscillations of a ^{4}He* Bose-Einstein condensate in an optical lattice at 1557.3 nm. Due to its low mass, metastable helium was efficiently accelerated orders of magnitude faster than demonstrated with other atoms. In a horizontal lattice, we could transfer a total of $800\hbar k$ of momentum by shuttling the atomic cloud back and forth 50 times between the $4\hbar k$ and $-4\hbar k$ momentum states with an efficiency of over 99% per Bloch cycle. In a vertical lattice, gravity-induced Bloch oscillations were demonstrated, from which the local gravitational acceleration was derived with a statistical uncertainty of 4×10^{-5}. A clear advantage of He* over other atoms is that it can be detected with a microchannel plate detector with near unity efficiency, and this enabled observation of Bloch oscillations up to 12 s even though the number of atoms decreased by three orders of magnitude. These results establish He* as a promising candidate for future precision measurements with atom interferometry.

DOI: 10.1103/PhysRevA.102.061302

Since the groundbreaking experiments by Kasevich and Chu [1,2], atom interferometry (AI) has become a fast growing field with many applications, ranging from gravimetry [3] to determinations of fundamental constants [4]. Most recently, also dark matter searches and gravitational wave detectors based on AI have been proposed [5–8]. Atom interferometry with ultracold samples is currently the most precise tool for measuring the atomic recoil velocity [9,10] induced by the absorption of one or more photons. From such measurements, a competitive value for the fine-structure constant α can be derived. This enables a comparison with a value of α obtained from measurements of the electron g factor [11], combined with high-level quantum electrodynamics (QED) calculations [12], thus providing a consistency check between different domains of physics.

The precision of AI is significantly improved by the transfer of multiple recoil momenta using so-called Bloch oscillations (BOs) [13,14]. Bloch oscillations occur when particles confined to a periodic potential are subjected to an external force. Under these circumstances, the motion of particles is oscillatory instead of uniform, as was first pointed out by Bloch [15] and Zener [16]. Bloch oscillations of cold atoms in periodic potentials formed by optical lattices were first studied by Ben Dahan *et al.* [17] and Wilkinson *et al.* [18]. Peik *et al.* [19] gave a quantum-optical interpretation of this effect in terms of photon exchanges between the atoms and the laser fields, showing that Bloch oscillations are equivalent to a sequence of rapid adiabatic passages between momentum states. Importantly, BOs provide a way to efficiently accelerate atoms by coherently transferring a well-controlled, large number of photon momenta, which have been used to increase the resolution of recoil measurements with cesium and rubidium atoms [9,10].

It was recently suggested that metastable helium (He*) (which can be made into a Bose-Einstein condensate [20]) is a promising candidate for atom interferometry experiments [21], for several reasons: Due to its low mass, it can be accelerated fast and efficiently, allowing fast separation of finite-size wave packets and easy detection of different momentum states. For example, helium atoms that differ by two-photon momenta separate 20 times faster than rubidium. The high internal energy of 20 eV of He* enables a near-unity detection efficiency with a microchannel plate detector, even for large dilute samples, increasing signal over other detection techniques such as absorption imaging and laser-induced fluorescence. Position-sensitive detectors can be used to make a full three-dimensional reconstruction of the atomic cloud [22,23] which helps to diagnose systematic effects. Another advantage of He* is its low second-order Zeeman shift of 2.3 mHz/G^2 [21] (2 times smaller than for ^{88}Sr and $\sim 10^5$ times smaller than for Rb and Cs [24,25]), relaxing the required magnetic field control. For recoil measurements, an added advantage is that the mass of helium is known with a 20 times higher accuracy than that of Rb, Cs, or Sr [26,27]. Finally, helium is one of the few atoms where the level structure can be calculated from first principles, enabling tests of QED theory.

In this work, we demonstrate first steps towards interferometry with a helium Bose-Einstein condensate (BEC). In particular, we show efficient and fast momentum transfer via Bloch oscillations in an optical lattice and demonstrate the enhanced sensitivity offered by a microchannel-plate-detector–based detection scheme that is unique to He*.

*Present address: QUANTUM, Institut für Physik, Universität Mainz, Staudingerweg 7, 55128 Mainz, Germany.

†W.V. initiated this work. Sadly, he passed away before it could be completed.

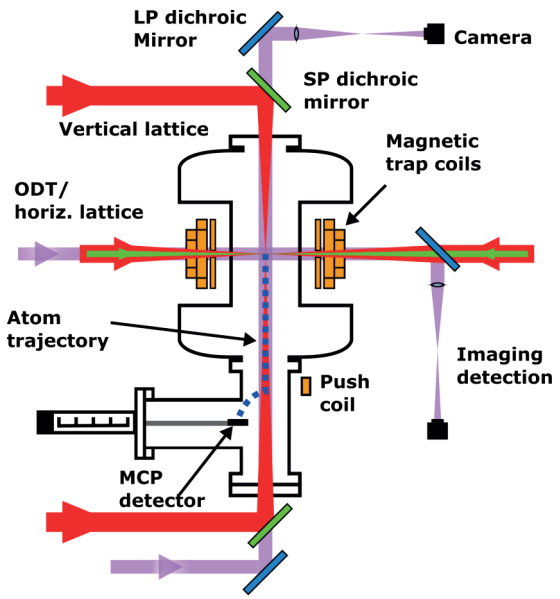

FIG. 1. Schematic of the experimental setup (not to scale) showing a cross section of the science chamber with the horizontal and vertical lattices (1557 nm) in red, the crossed optical dipole trap (ODT) (1557 nm) in green, and the imaging beams (1083 nm) in purple. Metastable helium atoms are evaporatively cooled in the ODT, resulting in a BEC of 5×10^6 atoms. Atoms are detected using absorption imaging or by dropping the atoms onto a microchannel plate (MCP) that is mounted 245 mm below the trap center. The different wavelengths are overlapped and separated by longpass and shortpass dichroic mirrors (LP and SP, respectively).

Our experimental apparatus to create a He* BEC is similar to the one described in [28]. Figure 1 shows the interaction chamber, including part of the optical setup and a cross section of the coils used for creating the required magnetic fields. We make use of a crossed optical dipole trap (ODT) in which the BEC is made and stored. The ODT is generated by two laser beams (450 mW each) derived from a single-laser system at 1557.3 nm (a master oscillator RFLSA GEN III from NP Photonics Inc. combined with a fiber amplifier NUA-1550-PB-0010-C2 from Nufern). Typically, our condensate consists of about 5×10^6 atoms and the condensate fraction is 90%.

The BEC can be detected by either absorption imaging using the time-of-flight technique or by letting the atoms fall onto a microchannel plate (MCP) detector after releasing the cloud. Absorption images are recorded by shining light resonant with the $2\,^3S_1$–$2\,^3P_2$ transition near 1083 nm (shown in purple in the figure) onto a InGaAs camera (Xeva-2.5-320 from Xenics), with a pixel size of 30 μm. To detect He* directly, an MCP detector (Hamamatsu, model No. F4655) is placed 245 mm below the trap. It can be shifted 20 mm out of the center to allow vertical lattice beams to pass. Atoms falling under gravity are pushed towards the MCP by briefly pulsing a current through a magnetic-field coil positioned just above the MCP.

In order to induce Bloch oscillations, we create an optical lattice potential with two counterpropagating beams that are derived from the same fiber amplifier as the ODT beams. Independent control of the power and timing of the ODT and lattice beams is achieved by using a distribution system of four acousto-optic modulators (AOMs) (Gooch-Housego). For experiments in the horizontal one-dimensional lattice, the lattice beams are overlapped with one of the ODT beams using a polarizing beam splitter. The $1/e^2$ waists of the lattice beams are set to 200 μm, approximately two times larger than the ODT. The AOMs used for lattice beam frequency control are driven by RF signals produced with direct-digital-synthesizer boards (Analog Devices AD9954) combined with homemade RF amplifiers. This system enables us to ramp the RF up or down with a speed well above 1 GHz/s, as needed to induce fast BOs. Bloch oscillations in the horizontal lattice configuration are induced by a linear frequency ramp of one of the lattice beams.

The effective acceleration of the lattice is equal to

$$a = \frac{\lambda}{2}\frac{d\Delta\nu(t)}{dt}, \tag{1}$$

where λ is the lattice laser wavelength and $\Delta\nu(t)$ is the frequency difference between the two lattice beams [19]. When viewed in the context of adiabatic transitions in the first Brillouin zone, the probability for an atom to successfully coaccelerate with the lattice is given by the Landau-Zener relation [29]

$$P^N = [\eta(1 - e^{a_c/a})]^N, \tag{2}$$

where η denotes the technical efficiency (losses due to frequency or timing imperfections), N is the number of BOs (each transferring two-photon momenta), and a_c is the critical acceleration of He*, which is given by [29]

$$a_c = \frac{\pi\hbar^2k^3}{64m_{\mathrm{He}}^2}\left(\frac{U_0}{E_R}\right)^2, \tag{3}$$

with m_{He} the atomic mass of ^{4}He* and $E_R = \frac{\hbar^2k^2}{2m_{\mathrm{He}}}$ the one-photon recoil energy, containing the reduced Planck constant $\hbar$, wave number $k = 2\pi/\lambda$, and potential depth U_0.

Figures 2(a) and 2(b) show absorption images of atoms in the horizontal plane after an expansion time of 5 ms, illustrating the momentum distribution of the atoms after being subjected to an accelerated optical lattice with a depth $1.25E_R$ moving towards the right. In Fig. 2(a), the frequency difference between the two lattice beams is chirped from 0 to 660 kHz in 1.4 ms, resulting in an acceleration of about 370 m/s^2. In Fig. 2(b), the frequency is chirped in 0.7 ms, resulting in an acceleration of about 730 m/s^2. Figure 2(c) shows a 0.2-ms chirp, or 2600 m/s^2. As observed from Fig. 2(a), the efficiency at low acceleration is near unity, resulting in a bright feature at a position corresponding to atoms that have been given a momentum of $8\hbar k$ (i.e., a velocity of 8×6.4 cm/s). At higher acceleration, not all atoms can follow the lattice, leading to a series of features revealing the discrete momentum states separated by $2\hbar k$, as shown in Fig. 2(b). At even higher acceleration, the efficiency becomes very small and most atoms remain in the $0\hbar k$ state, as shown in Fig. 2(c).

The acceleration efficiency is quantified in Fig. 2(d), showing the fraction of atoms that are successfully coaccelerated with the lattice to $8\hbar k$, as a function of the lattice acceleration. The orange line in Fig. 2(d) shows a fit of Eq. (2) to the data using $N = 4$, yielding $\eta = 0.980(3)$ and $a_c = 1294(41)$ m/s^2.

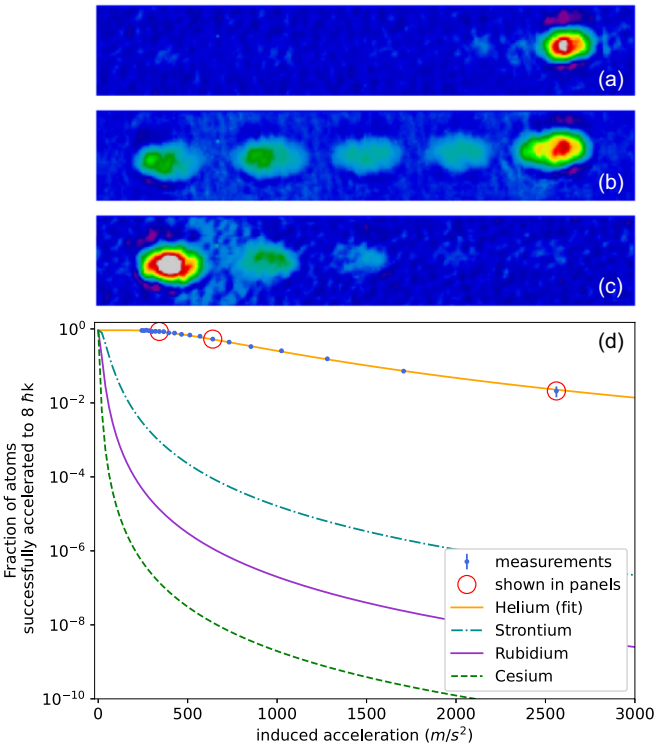

FIG. 2. Absorption images of the atoms in the horizontal plane after an expansion time of 5 ms showing atoms in (from left to right) momentum states 0 $\hbar k$ to 8 $\hbar k$ due to a lattice acceleration of (a) 370 m/s^2, (b) 730 m/s^2, and (c) 2600 m/s^2, in an optical lattice with a depth $1.25E_R$. (d) The blue data points show the number of atoms that accelerated to $8\hbar k$ relative to the total number of atoms, the yellow line is a fit of P^4 [Eq. (3)] (details in text), and the red circles show the data points related to the image panels. Theoretical curves for other atomic species are shown, assuming equal lattice depth but lattice wavelengths commonly used for those species [6,10,30]. Note that equal lattice depth does not mean equal power. With modest laser power, deep lattices have been obtained for Rb and Cs by operating the lattice near resonance, at the expense of losses due to the increased scattering rate.

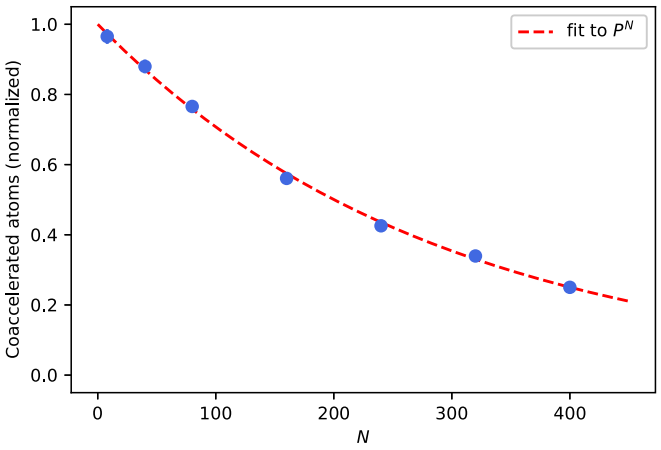

FIG. 3. Normalized number of atoms that have been successfully coaccelerated with the lattice as a function of N, obtained from absorption measurements. The atoms were accelerated and decelerated back and forth with 8 BOs at a time, to a maximum of 400 BOs. The red fit [Eq. (2)] with $a = 2845.33$ m/s^2 and $a_c = 42\,944.1$ m/s^2 (deduced from depth calibration using Rabi oscillations) yields an efficiency $\eta = 0.996\,54(6)$.

The fitted critical acceleration is in excellent agreement with $a_c = 1287(9)$ m/s^2, the value found from Eq. (3) with the depth of the lattice derived from a measurement of the Rabi frequency of the atoms in the lattice moving with a velocity of $\hbar k/m_{\mathrm{He}}$. The blue, purple, and green lines show calculations for ^{88}Sr, ^{87}Rb, ^{133}Cs, assuming similar depths for lattices operating at 532, 780, and 866 nm, respectively [6,10,30], illustrating the relative ease by which helium can be rapidly and efficiently accelerated.

Due to the Gaussian beam shape of the lattice beams, atoms near the center are more efficiently accelerated than those in the wings. As a consequence, the efficiency of the first few cycles is lower than that of the subsequent steps. We have also performed measurements where atoms are driven back and forth between the $-4\hbar k$ and $4\hbar k$ momentum states, by applying a triangular frequency chirp to the lattice AOMs, transferring a total of $800\hbar k$. Figure 3 shows the number of atoms that have been successfully coaccelerated with the lattice as a function of N. Here a lattice depth of approximately $7.3E_R$ and a lattice acceleration of 2.86×10^3 m/s^2 were used. From this measurement an efficiency of 0.996 54(7) per oscillation was derived, comparable to efficiencies found in other experiments (see, for instance, [31]). Note that, for helium, far fewer BOs are needed to achieve a certain velocity than for heavier atoms.

We now turn to Bloch oscillations in the vertical plane. In the vertical direction, earth's gravity provides a constant force along the direction of the lattice, giving rise to BOs, even when the lattice itself is kept stationary [6]. The relation between the oscillation period T_{Bloch} and the gravitational acceleration g is given by

$$T_{\mathrm{Bloch}} = \frac{2\hbar k}{m_{\mathrm{He}} g}, \tag{4}$$

which in the case of helium in our lattice is roughly 13 ms. Therefore, by measuring the frequency of the gravity-induced Bloch oscillations, g can be measured directly [6]. Note that more elaborate schemes that combine BOs and AI techniques have resulted in an improvement of the sensitivity by several orders of magnitude [30].

Figure 4 shows the atomic cloud after release from the lattice using either absorption imaging after a 5-ms expansion time [Fig. 4(a)] or detection on an MCP detector [Fig. 4(c)], revealing the discretized momentum distribution of the cloud. The time the atoms have spent in the vertical lattice is given in the panels. To infer the mean momentum of the atomic cloud at the moment of release, we determine either the mean position of the atoms on the absorption images [blue data points in Fig. 4(b)] or the mean arrival time of the atoms on the MCP detector [blue data points in Fig. 4(d)], showing the characteristic sawtooth behavior expected of Bloch oscillations [17,18]. Each data point is the average of three measurements. The error bars show the standard deviation of the mean, which is determined by the number of atoms and their momentum spread, i.e., the phase-space density of the

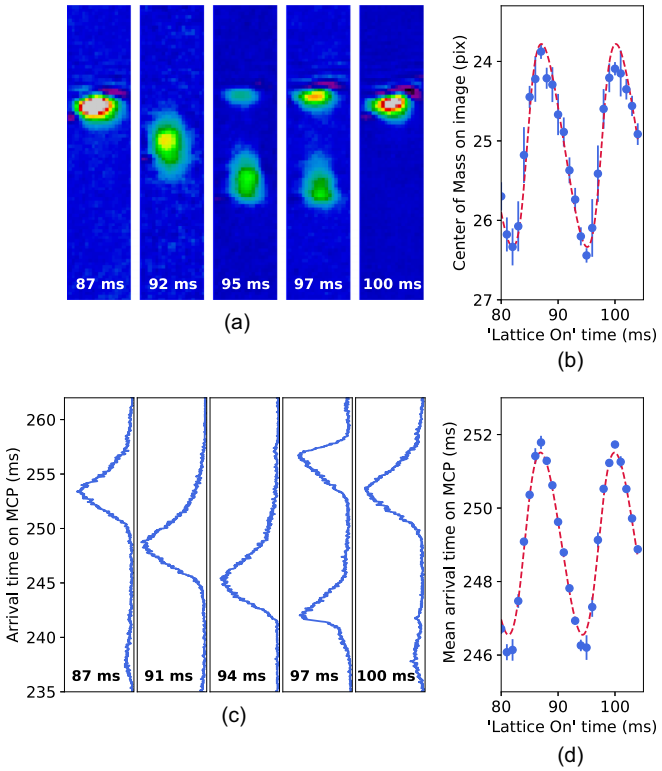

FIG. 4. (a) Absorption image of the atoms in the vertical plane after an expansion time of 5 ms showing Bloch oscillations under gravity. The time that the atoms spent in the lattice for each measurement is given in each panel. (b) Mean position of the atoms derived from absorption images as a function of the time spent in the lattice (blue data points). (c) Signal observed on the MCP detector after release showing Bloch oscillations under gravity. (d) Mean arrival time of the atoms derived from the MCP traces as a function of time spent in the lattice (blue data points). The red curves in (b) and (d) follow from a band-structure model.

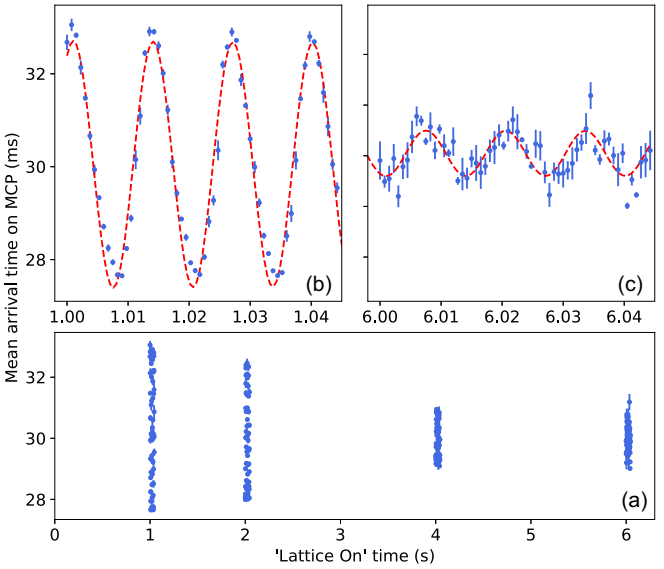

FIG. 5. (a) Mean arrival time of the atoms falling onto the MCP detector as a function of time spent in the lattice ($0.5E_R$), showing Bloch oscillations due to gravity in a lattice. Also shown are close-ups of Bloch oscillations after (b) 1 s and (c) 6 s in the lattice. The red line shown in (b) and (c) is the result of a sinusoidal fit to the data in (a), yielding $g = 9.7946(4)$ m/s^2 (statistical error only).

sample. This is the motivation for performing these experiments with a Bose-Einstein condensate. The red curves shown in Figs. 4(b) and 4(d) follow from a band-structure model [19] with the input parameters chosen to match the data. Note that the measurements shown in Figs. 4(b) and 4(d) are related to the momentum distribution of the cloud and hence are not sensitive to shot-to-shot fluctuations of the number of atoms. For the data shown in Fig. 4, the error obtained with absorption imaging is about 2 times larger than that with the MCP. However, this factor depends strongly on the number of atoms in the sample and (related to that) the voltage that is applied to the MCP detector. Note that all measurements in Fig. 5 have been taken at a constant MCP voltage. The number of atoms that remain trapped in the lattice decreases rapidly due to the weak radial confinement. With absorption imaging, no distinguishable signal is observed after 2 s, whereas with the MCP detector, a clear signal is observed for up to 6 s, at which point the number of atoms has decreased by at least an order of magnitude. Oscillation times up to 12 s (not shown) have been observed by applying higher voltages to the MCP. Counting the signal from individual He* atoms instead of simply measuring the current will likely further extend the time at which the atoms can still be observed [22,23].

Figure 5 shows the mean arrival time of the atoms falling onto the MCP detector for much longer times spent in the lattice ($0.5E_R$). A clearly measurable contrast up to 6 s is obtained in which time the atoms have made over 450 consecutive Bloch oscillations. Figures 5(b) and 5(c) show a close-up of the data. There are noticeable damping effects on the BO, which are attributed to three sources of rather different physical origin. (i) Gustavsson *et al.* [32] have shown that atom-atom interactions in a dense BEC lead to dephasing immediately after release of the cloud. In our measurements, we have minimized these effects by reducing the number of atoms through the introduction of a 5-s "hold time" before transferring the atoms to the lattice, at the cost of a reduced signal-to-noise ratio. Note that it was recently pointed out that atom-atom interactions in a BEC can be used to generate useful entanglement to improve the measurements below the shot-noise limit [33], which could directly be implemented in our experiment. (ii) When the atom number is low, electronic (detector) noise reduces the apparent contrast. This can be avoided by counting the signal from individual atoms [22,23]. (iii) As discussed by Ferrari *et al.* [6], vibrations of the mirrors and fibers will lead to dephasing. In our setup, we use two separate beam paths to create an optical lattice (instead of a retroreflector) which makes our measurement sensitive to vibrations. We observe that the dephasing is particularly dependent on the alignment of the two lattice beams, which varies from day to day. Increasing the waist of our lattice will likely reduce this effect.

Due to the dephasing, the observed shape of the Bloch oscillation changes from a sawtooth to a sinelike function. This distortion would have to be minimized and modeled for

a proper absolute measurement of g from this signal, which is beyond the scope of this paper. In order to still obtain a statistical uncertainty estimate of our gravity measurement demonstration, we have fitted an (exponentially decaying) sinusoidal function to the data in Fig. 5(a), shown as the red line in Figs. 5(b) and 5(c). This fit yields $g = 9.7946(4)$ m/s^2, i.e., a statistical uncertainty for a determination of g of 4×10^{-5}.

In conclusion, we have demonstrated Bloch oscillations with a metastable helium BEC. Due to its low mass, helium can be efficiently accelerated to high velocities, which makes it a particularly interesting candidate for experiments that benefit from splitting the atomic wave function over large distances [13,14,34–36]. Our measurements illustrate the high signal-to-noise ratio that can be obtained using an MCP detector for long-term observation of Bloch oscillations. As a result of its low mass, the observed Bloch oscillations of helium are distinct from those of heavier atoms; the gravity-induced Bloch oscillations in our vertical lattice have a frequency of only 73 Hz, while the characteristic length scale of the motion of the atoms is as large as 200 μm [37]. This long length scale allows us to accurately determine the influence of a laser beam that is focused at the apex of the trajectories [38]. Use of this method to measure the tune-out wavelengths of He as a precise test of quantum-electrodynamic calculations [39] is left for future work.

The authors would like to thank Prof. T. van Leeuwen of the Eindhoven University of Technology and Dr. M. D. Hoogerland from the University of Auckland for technical and material support. We are grateful for many stimulating discussions with Y. van der Werf and Dr. R. Jannin. We thank Prof. Wim Ubachs for support. This work was financially supported by the Dutch Foundation for Fundamental Research on Matter (FOM).

[1] M. A. Kasevich and S. Chu, Phys. Rev. Lett. **67**, 181 (1991).
[2] M. A. Kasevich and S. Chu, Appl. Phys. B **54**, 321 (1992).
[3] V. Ménoret, P. Vermeulen, N. Le Moigne, S. Bonvalot, P. Bouyer, A. Landragin, and B. Desruelle, Sci. Rep. **8**, 12300 (2018).
[4] G. Rosi, F. Sorrentino, L. Cacciapuoti, and G. Tino, Nature (London) **510**, 518 (2014).
[5] D. O. Sabulsky, I. Dutta, E. A. Hinds, B. Elder, C. Burrage, and E. J. Copeland, Phys. Rev. Lett. **123**, 061102 (2019).
[6] G. Ferrari, N. Poli, F. Sorrentino, and G. M. Tino, Phys. Rev. Lett. **97**, 060402 (2006).
[7] S. Dimopoulos, P. W. Graham, J. M. Hogan, M. A. Kasevich, and S. Rajendran, Phys. Rev. D **84**, 028102 (2011).
[8] B. Canuel *et al.*, Sci. Rep. **8**, 14064 (2018).
[9] R. Bouchendira, P. Cladé, S. Guellati-Khélifa, F. Nez, and F. Biraben, Phys. Rev. Lett. **106**, 080801 (2011).
[10] R. H. Parker, C. Yu, W. Zhong, B. Estey, and H. Müller, Science **360**, 191 (2018).
[11] D. Hanneke, S. Fogwell Hoogerheide, and G. Gabrielse, Phys. Rev. A **83**, 052122 (2011).
[12] T. Aoyama, T. Kinoshita, and M. Nio, Phys. Rev. D **97**, 036001 (2018).
[13] P. Cladé, S. Guellati-Khélifa, F. Nez, and F. Biraben, Phys. Rev. Lett. **102**, 240402 (2009).
[14] H. Müller, S.-w. Chiow, S. Herrmann, and S. Chu, Phys. Rev. Lett. **102**, 240403 (2009).
[15] F. Bloch, Z. Phys. **52**, 555 (1929).
[16] H. Jones and C. Zener, Proc. R. Soc. London Ser. A **144**, 101 (1934).
[17] M. Ben Dahan, E. Peik, J. Reichel, Y. Castin, and C. Salomon, Phys. Rev. Lett. **76**, 4508 (1996).
[18] S. R. Wilkinson, C. F. Bharucha, K. W. Madison, Q. Niu, and M. G. Raizen, Phys. Rev. Lett. **76**, 4512 (1996).
[19] E. Peik, M. Ben Dahan, I. Bouchoule, Y. Castin, and C. Salomon, Phys. Rev. A **55**, 2989 (1997).
[20] F. Pereira Dos Santos, J. Léonard, J. Wang, C. J. Barrelet, F. Perales, E. Rasel, C. S. Unnikrishnan, M. Leduc, and C. Cohen-Tannoudji, Phys. Rev. Lett. **86**, 3459 (2001).
[21] W. Vassen, R. P. M. J. W. Notermans, R. J. Rengelink, and R. F. H. J. van der Beek, Appl. Phys. B **122**, 289 (2016).
[22] T. Jeltes, J. McNamara, W. Hogervorst, W. Vassen, V. Krachmalnicoff, M. Schellekens, A. Perrin, H. Chang, D. Boiron, A. Aspect, and C. Westbrook, Nature (London) **445**, 402 (2007).
[23] W. Vassen, C. Cohen-Tannoudji, M. Leduc, D. Boiron, C. I. Westbrook, A. Truscott, K. Baldwin, G. Birkl, P. Cancio, and M. Trippenbach, Rev. Mod. Phys. **84**, 175 (2012).
[24] R. P. del Aguila, T. Mazzoni, L. Hu, L. Salvi, G. M. Tino, and N. Poli, New J. Phys. **21**, 019502 (2019).
[25] D. Steck, http://www.steck.us/alkalidata (2019).
[26] P. J. Mohr, D. B. Newell, and B. N. Taylor, Rev. Mod. Phys. **88**, 035009 (2016).
[27] M. Wang, G. Audi, F. G. Kondev, W. J. Huang, S. Naimi, and X. Xu, Chin. Phys. C **41**, 030003 (2017).
[28] R. van Rooij, Frequency metrology in quantum degenerate helium, Ph.D. thesis, Vrije Universiteit, 2012.
[29] P. Cladé, Atomic interferometry, in *Proceedings of the International School of Physics "Enrico Fermi," Course CLXXXVIII, Varenna, 2013*, edited by G. M. Tino and M. A. Kasevich (IOS, Amsterdam, 2013), pp. 237–244.
[30] M. Andia, R. Jannin, F. Nez, F. Biraben, S. Guellati-Khélifa, and P. Cladé, Phys. Rev. A **88**, 031605(R) (2013).
[31] P. Cladé, E. de Mirandes, M. Cadoret, S. Guellati-Khélifa, C. Schwob, F. Nez, L. Julien, and F. Biraben, Phys. Rev. Lett. **96**, 033001 (2006).
[32] M. Gustavsson, E. Haller, M. J. Mark, J. G. Danzl, G. Rojas-Kopeinig, and H.-C. Nägerl, Phys. Rev. Lett. **100**, 080404 (2008).
[33] S. S. Szigeti, S. P. Nolan, J. D. Close, and S. A. Haine, Phys. Rev. Lett. **125**, 100402 (2020).
[34] T. Kovachy, P. Asenbaum, C. Overstreet, C. A. Donnelly, S. M. Dickerson, A. Sugarbaker, J. M. Hogan, and M. A. Kasevich, Nature (London) **528**, 530 (2015).
[35] G. Rosi, G. D'Amico, L. Cacciapuoti, F. Sorrentino, M. Prevedelli, M. Zych, Č. Brukner, and G. M. Tino, Nat. Commun. **8**, 15529 (2017).

[36] P. Asenbaum, C. Overstreet, T. Kovachy, D. D. Brown, J. M. Hogan, and M. A. Kasevich, Phys. Rev. Lett. **118**, 183602 (2017).

[37] Note that with lithium atoms, Bloch oscillations with frequencies as low as 20 Hz and length scales of 300 μm have been obtained by applying a magnetic field gradient along the lattice direction; see Z. A. Geiger, K. M. Fujiwara, K. Singh, R. Senaratne, S. V. Rajagopal, M. Lipatov, T. Shimasaki, R. Driben, V. V. Konotop, T. Meier, and D. M. Weld, Phys. Rev. Lett. **120**, 213201 (2018).

[38] O. Onishchenko, R. F. H. J. van der Beek, R. Jannin, Y. van der Werf, K. S. E. Eikema, and H. L. Bethlem (unpublished).

[39] B. M. Henson, R. I. Khakimov, R. G. Dall, K. G. H. Baldwin, L.-Y. Tang, and A. G. Truscott, Phys. Rev. Lett. **115**, 043004 (2015).